



Dedicated to innovation in aerospace

NLR-TP-2017-096 | April 2017

Pushing Ahead - SUPRA Airplane Model for Upset Recovery

CUSTOMER: European Commission



NLR – Netherlands Aerospace Centre

Netherlands Aerospace Centre

NLR is a leading international research centre for aerospace. Bolstered by its multidisciplinary expertise and unrivalled research facilities, NLR provides innovative and integral solutions for the complex challenges in the aerospace sector.

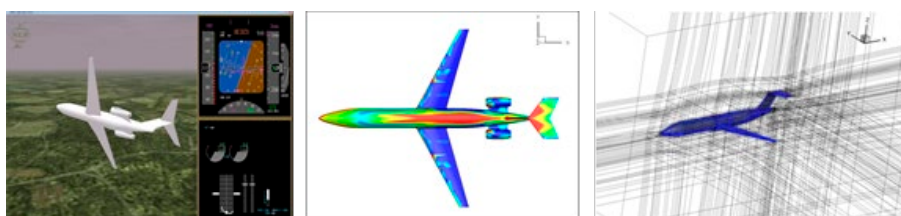
NLR's activities span the full spectrum of Research Development Test & Evaluation (RDT & E). Given NLR's specialist knowledge and facilities, companies turn to NLR for validation, verification, qualification, simulation and evaluation. NLR thereby bridges the gap between research and practical applications, while working for both government and industry at home and abroad.

NLR stands for practical and innovative solutions, technical expertise and a long-term design vision. This allows NLR's cutting edge technology to find its way into successful aerospace programs of OEMs, including Airbus, Embraer and Pilatus. NLR contributes to (military) programs, such as ESA's IXV re-entry vehicle, the F-35, the Apache helicopter, and European programs, including SESAR and Clean Sky 2.

Founded in 1919, and employing some 650 people, NLR achieved a turnover of 71 million euros in 2016, of which three-quarters derived from contract research, and the remaining from government funds.

For more information visit: www.nlr.nl

Pushing Ahead - SUPRA Airplane Model for Upset Recovery



Problem area

Loss of control in flight (LOC-I) is the leading cause of fatal accidents in commercial aviation today. During a LOC-I event, the aircraft often enters an unusual attitude or upset condition, for instance during a stall, which would otherwise not be encountered in normal operations. Existing simulation facilities are limited in their ability to reproduce the environment of a stall or upset. The Simulation of Upset Recovery in Aviation (SUPRA) project, a European 7th Framework Programme project, researched extending the aerodynamic models for simulators and investigated the modification of hexapod and centrifuge-based simulators that are used for upset recovery training. Representative simulation of post stall airplane dynamics was studied aimed to facilitate pilot training for upset recognition, prevention and recovery.

Description of work

Within the SUPRA project an aerodynamic model in extended flight envelope, including stall and post-stall conditions, was developed to provide representative behaviors in lateral/directional departure, post stall gyration and spin for a conventional twin-engine commercial transport configuration. This paper presents the SUPRA simulation environment which includes the aerodynamic model in extended flight envelope complemented with a command and stability augmentation system and buffeting model for providing acceptable handling

REPORT NUMBER

NLR-TP-2017-096

AUTHOR(S)

M.H. Smaili
B.I. Soemarwoto
N.B. Abramov
M.G. Goman
A.N. Khrabrov
E.N. Kolesnikov
L. Fucke

REPORT CLASSIFICATION

UNCLASSIFIED

DATE

April 2017

KNOWLEDGE AREA(S)

Safety
Flight Operations
Training, Mission
Simulation and Operator
Performance
Computational Physics and
Theoretical Aerodynamics

DESCRIPTOR(S)

loss of control
upset recovery
computational
aerodynamics
flight simulation
aircraft stall

qualities in the normal flight envelope and natural stall warning, respectively. The main requirement for the SUPRA aerodynamic model is that it should reflect major nonlinear aerodynamic phenomena at high angles of attack and be representative in a sense that pilots can be exposed to various aircraft dynamic behaviors associated with instability and loss of control due to stall and flow separation.

Results and conclusions

The SUPRA aerodynamic model was successfully validated by a number of expert pilots and found acceptable for upset recovery training. The piloted evaluation trials at NLR's GRACE, TNO's Desdemona, and TsAGI's PSPK-102, provided proof that the SUPRA model behavior is representative of a jet transport of conventional configuration, inside and outside the normal flight envelope. Important arguments have been gathered in support of the usability of the applied phenomenological modeling approach for stall simulation. SUPRA provided evidence that the method, which had previously been used successfully for the prediction of stall and spin behavior of advanced fighter jet configurations, is usable to produce an all-envelope class-representative model. The model's re-configurability allows for customization to reproduce aircraft type-specific characteristics.

Applicability

The SUPRA aerodynamic stall model is applicable, as a possible add-on, to current simulator databases for improved upset prevention and recovery training. The generic model is representative of a medium range two engine transport aircraft with low tail or high tail configuration.

The SUPRA project was funded by the 7th European Union Framework Programme (FP7/2007-2013) under Grant Agreement no. 233543.

GENERAL NOTE

This report is based on a presentation held at the AIAA Modeling and Simulation Technologies Conference, Minneapolis, MN, August 13-16, 2012.

Front cover courtesy of Telegraaf.

NLR

Anthony Fokkerweg 2
1059 CM Amsterdam

p) +31 88 511 3113 f) +31 88 511 3210

e) info@nlr.nl i) www.nlr.nl



Dedicated to innovation in aerospace

NLR-TP-2017-096 | April 2017

Pushing Ahead - SUPRA Airplane Model for Upset Recovery

CUSTOMER: European Commission

AUTHOR(S):

M.H. Smaili

NLR

B.I. Soemarwoto

NLR

N.B. Abramov

De Montfort University

M.G. Goman

De Montfort University

A.N. Khrabrov

TsAGI

E.N. Kolesnikov

TsAGI

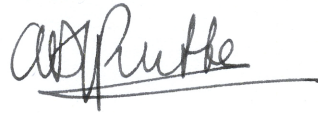
L. Fucke

Boeing Research & Technology Europe

This report is based on a presentation held at the AIAA Modeling and Simulation Technologies Conference, Minneapolis, MN, August 13-16, 2012.

The contents of this report may be cited on condition that full credit is given to NLR and the author(s).

CUSTOMER	European Commission
CONTRACT NUMBER	233543
OWNER	NLR + partner(s)
DIVISION NLR	Aerospace Operations
DISTRIBUTION	Unlimited
CLASSIFICATION OF TITLE	UNCLASSIFIED

APPROVED BY :															
AUTHOR				REVIEWER				MANAGING DEPARTMENT							
M.H. Smaili 				External reviewers				A.D.J. Rutten 							
DATE	9	0	3	17	DATE					DATE	0	4	0	4	17

Contents

Nomenclature	5
I. Introduction	6
II. SUPRA simulation model	7
A. Aerodynamic phenomena in extended envelope	7
B. Analytic approximations	8
C. Unsteady aerodynamic model	9
D. Complementary use of CFD	10
E. Command stability augmentation system	12
F. Propulsion model	12
G. Buffeting model	12
III. Nonlinear Dynamics Analysis	13
A. Departure Criteria	13
B. Nonlinear bifurcation analysis	14
IV. Aerodynamic model validation and parameters tuning	15
A. Methods	15
B. Results	16
V. Conclusions	16
Acknowledgments	17
References	17

This page is intentionally left blank.

Pushing Ahead - SUPRA Airplane Model for Upset Recovery

N.B.Abramov¹ and M.G.Goman²
De Montfort University, Leicester, UK, LE1 9BH

A.N.Khrabrov³ and E.N.Kolesnikov⁴
Central Aerohydrodynamic Institute TsAGI, Zhukovsky, Russia, 140160

L.Fucke⁵
Boeing Research & Technology Europe, Madrid, Spain.

B.Soemarwoto⁶ and H.Smaili⁷
National Aerospace Laboratory (NLR), Anthony Fokkerweg 2, 1059 CM Amsterdam, The Netherlands.

One of the primary objectives of the European Union 7th Framework Program research project SUPRA – “Simulation of Upset Recovery in Aviation” – is the development and validation of the aerodynamic model of a generic large transport airplane aimed for piloted simulation in the post-stall region and upset recovery training. Modeling methods for prediction of post-stall flight dynamics, use of the wind tunnel data from different experimental facilities complemented by CFD analysis, validation criteria, nonlinear dynamics investigation and piloted simulation results are presented in this paper. The aerodynamic model was successfully validated by a number of expert pilots and found acceptable for upset recovery training.

Nomenclature

V, α, β	= speed, angles of attack and sideslip
θ, ϕ, ψ	= pitch, roll and yaw angles
p, q, r	= projections of angular velocity vector onto body-axis reference frame
p_a, q_a, r_a	= projections of angular velocity vector onto wind-axis reference frame
$\omega = p_a$	= projection of angular velocity vector onto speed vector
\mathbf{F}, \mathbf{M}	= aerodynamic force and moment vectors
$\delta_e, \delta_a, \delta_r$	= elevator, aileron and rudder deflections
$X_{lon}, X_{lat}, X_{ped}$	= pilot control inputs
H	= altitude
n_x, n_y, n_z	= projections of the load factor vector on wind-fixed reference frame
b	= wing span
CSAS	= command and stability augmentation system
AoA	= angle of attack
SUPRA	=Simulation of Upset Recovery in Aviation

¹Senior Research Fellow, Department of Engineering, The Gateway, AIAA Member.

²Professor, Department of Engineering, The Gateway, AIAA Senior Member

³Head of Division, Flight Dynamics and Control Systems Department

⁴Research Fellow, Flight Dynamics and Control Systems Department

⁵Senior Engineer, Safety R&D, Adv. Sur del Aeropuerto de Barajas, 38, 28042, AIAA Member, SAE Member

⁶Research Scientist, Flight Physics and Loads

⁷Aerospace Engineer, Training Human Factors and Cockpit Operations Department, AIAA Member

I. Introduction

The loss of control in flight (LOC-I) is currently the number-one threat to aviation safety and there is a general opinion that improvement in safety can be done via pilot training on available full flight simulators (<http://icatee.org>). Today's flight simulators are not totally adequate for this mission due to limitations of aerodynamic models and motion driving algorithms. The SUPRA research project – Simulation of Upset Recovery in Aviation – has been funded by the European Union 7th Framework Program to enhance the flight simulation envelope for upset recovery simulation. Within the project an aerodynamic model in extended flight envelope including stall and post-stall conditions was developed to provide representative behaviors in lateral/directional departure, post stall gyration and spin for a conventional twin-engine commercial transport configuration. Using this aerodynamic model new motion cuing solutions for both hexapod and centrifuge-based simulator platforms were developed¹.

This paper presents the SUPRA simulation environment which includes the aerodynamic model in extended flight envelope complemented with command and stability augmentation system and buffeting model for providing acceptable handling qualities in the normal flight envelope and natural stall warning, respectively. Representative simulation of post stall airplane dynamics is aimed to facilitate pilot training for upset recognition, prevention and recovery.

The backbone of the aerodynamic model includes the experimental wind tunnel data obtained in TsAGI for an airliner with two under-wing mounted engines and conventional tail². The aerodynamic data were obtained in low speed and transonic wind tunnels using different experimental facilities. Additional aerodynamic data were generated at NLR using CFD methods. The basic aircraft geometry for CFD study was a T-tail aircraft configuration derived from the NACRE model (New Aircraft Concepts REsearch) which was developed in the EU FP-6 NACRE project (2005-2009). The main requirement for the aerodynamic model is that it should reflect major nonlinear aerodynamic phenomena at high angles of attack and be representative in a sense that pilots can be exposed to various aircraft dynamic behaviors associated with instability and loss of control due to stall and flow separation. Section IIa presents how the experimental and computational data are processed and integrated in the SUPRA representative aerodynamic model.

Validation criteria for Level D certified Full Flight Simulators (FFS) require that the model output accurately matches aircraft responses measured in flight. Similar approach to validation of post-stall nonlinear airplane dynamics is more difficult and less reliable due to lack of available flight data and a nonlinear nature of aerodynamics and flight dynamics. Aircraft post-stall departure may have a random and unpredictable occurrence. At high angles of attack aircraft has multiple critical flight regimes and minor changes in control inputs can trigger dynamics development from one regime to another.

The SUPRA aerodynamic model was validated at high angles of attack region using comparison with dynamically scaled free-spinning model in vertical wind tunnel³. Parameters in developed spin and recovery control were in a good match with experimental data. Although Reynolds number may strongly affect aerodynamic characteristics in stall region, it is generally accepted that dynamically scaled free-spinning models in vertical wind tunnel serve as an effective instrument for investigation of spin modes and spin recovery procedures⁴. Effect of Reynolds number on aerodynamic autorotation and onset of aerodynamic asymmetry at stall conditions is a fundamental problem which should be addressed for adequate and realistic simulation of lateral/directional departure. Some preliminary CFD and low order aerodynamic models results related to this problem are presented and discussed in this paper.

As an important part of the validation process a systematic analysis of the SUPRA model nonlinear dynamics has been conducted to investigate a variety of airplane critical flight regimes. This study highlighted potential dangers following airplane departure, the character of post-stall gyration, incipient/developed spin modes and high speed steep spiral dive. A special study was made to investigate effect of a number of free parameters introduced in the aerodynamic model on airplane nonlinear dynamics, namely the post-stall lateral/directional departure and longitudinal deep-stall regimes.

The final validation of the SUPRA model was made in piloted simulation with participation of a number of experienced test and airline pilots on three flight simulators – Desdemona (TNO), Grace (NLR) and PSPK-102 (TsAGI). Feedback from pilots on representativeness of stall dynamics in qualitative and quantitative terms helped to tune reconfigurable parameters of the SUPRA model to improve its fidelity. The procedure and criteria for piloted validation and some results are summarized in Section IV.

II. SUPRA simulation model

The SUPRA airplane model was developed using MATLAB/Simulink[®] computing environment to ensure compatibility with flight simulators at TNO Desdemona, TsAGI PSPK-102 and NLR GRACE. The block-diagram of the SUPRA simulation model is shown in Fig. 1. The simulation model includes the block for computation of aerodynamic forces and moments with contribution from propulsion, equations of motion considering airplane as a rigid body, simple buffeting model imitating high frequency cockpit vibrations indicating approach to stall and basic command and stability augmentation system (CSAS) for shaping controllability and stability characteristics at normal flight regimes to meet requirements for handling qualities. In flight simulator the pilot perceives motion differently from that in real flight. The simulator motion cuing depends on kinematic constraints of flight simulator platform, visualization system and implemented motion driving algorithms¹. A realistic simulation of vestibular cues during intensive large amplitude motion following the lateral/directional departure is hardly possible, however realistic visual simulation can allow experienced pilot to validate simulated motions and tune the model parameters to improve model fidelity.

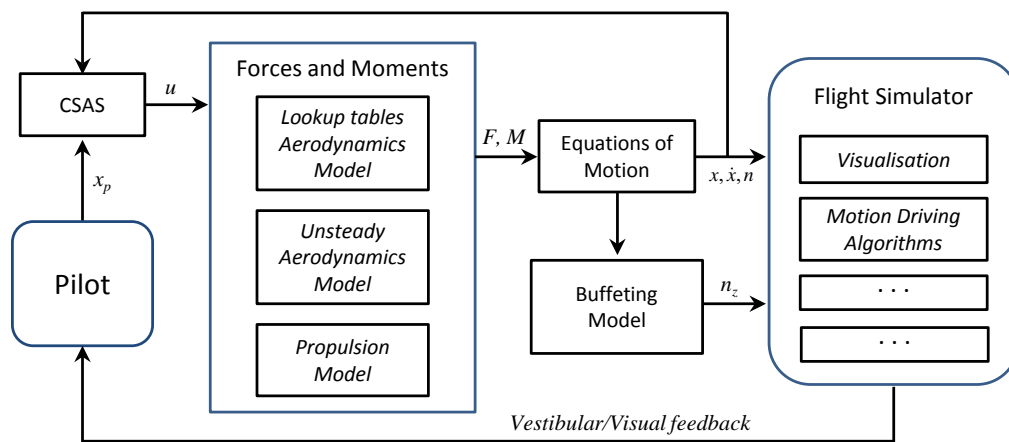


Figure 1. SUPRA simulation model structure

A. Aerodynamic phenomena in extended envelope

Analysis of upset-related flight accidents shows that upset events may advance through different phases dynamically evolving from safe ones to critically dangerous⁵. Upsets are associated with unusual attitudes with pitch and bank angles exceeding normally encountered in flight operations of transport aircraft. In case of incorrect recovery an unusual attitude can evolve into stall or situation when aircraft exceeds speed or g-limits. Both these situations being critically dangerous require special pilot training and this necessitates that an aerodynamic model should be extended to high angles of attack at low and high Mach numbers from take-off to cruise speeds of flight.

The aerodynamic model of a generic airplane configuration with two engines mounted under wing and conventional tail is developed for a wide range of angles of attack, sideslip and angular rate based on experimental data obtained in TsAGI's wind tunnels using static, forced oscillations and rotary balance tests (Fig. 2). Mach dependence for aerodynamic coefficients is tested in a wind tunnel in the limited range of angles of attack. Opposite, a wide range of angles of attack, sideslip ($-20 < \alpha < 90$ deg, $|\beta| < 30$ deg) and rate of rotation are investigated only for low Mach numbers. These tests include forced oscillations with small and large amplitudes and rotary balance measurements. Special procedures for combining available data obtained on different experimental facilities are required to allow the aerodynamic model in extended flight envelop to be smooth, consistent and valid in a wider region of flight parameters, for example, in the corner area between the high- and low-Mach number data, where stall is still possible within allowable structural limits.

Increase of angle of attack above some critical value leads to stall which is associated with onset of flow separation over an area of the wing^{2,6,7,8}. A sudden loss of lift and nonlinear transformation in the pitching moment coefficient are typical consequences of flow separation (Fig. 3). Stall conditions may produce strong dependence of the aerodynamic loads on prehistory of motion. Fig. 4 shows variation in the normal force coefficient in static conditions (filled circles) and during forced oscillations with a number of non-dimensional frequencies k and large amplitude of oscillations (empty markers). Increase of angle of attack leads to significant delay of flow separation and increase in maximum lift, while during decrease of angle of attack separated flow conditions are continued to lower angles of attack region. Such dynamic hysteresis can produce negative damping in the pitching moment. The above phenomena leads to a number of nonlinear effects in longitudinal dynamics such as g-break with altitude loss, dynamic instability in pitch, departure to deep stall regime. In the lateral/directional mode stall leads to deterioration of the rolling and yawing moment coefficients negatively affecting airplane stability and control effectiveness. Figs. 5 (rotary balance test) shows dependences of the yawing moment coefficient on angle of attack, sideslip and non-dimensional rate of rotation ω , so-called velocity vector roll rate. One can see significant nonlinearities in sideslip dependence, a similar dependence appears on rotation rate. Note that onset of directional instability $C_{n\beta} < 0$ at $30 < \alpha < 50^\circ$ occurs due to vertical tail shadowing by wings and fuselage.

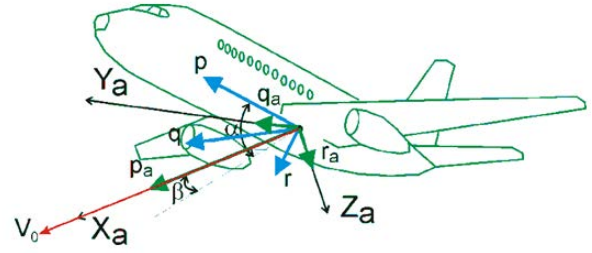


Figure 2. Generic transport airplane: body-axis and wind-axis reference frames.

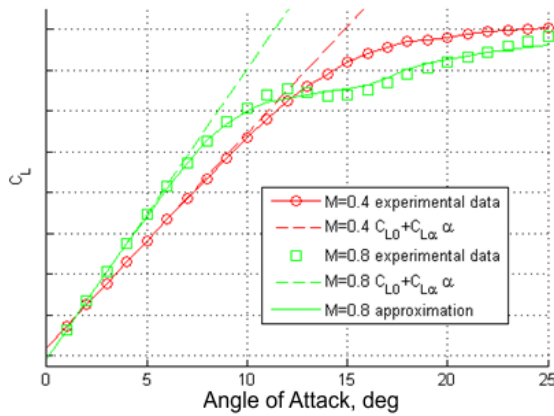


Figure 3. Lift coefficient: analytic approximation of angle of attack and Mach number dependencies.

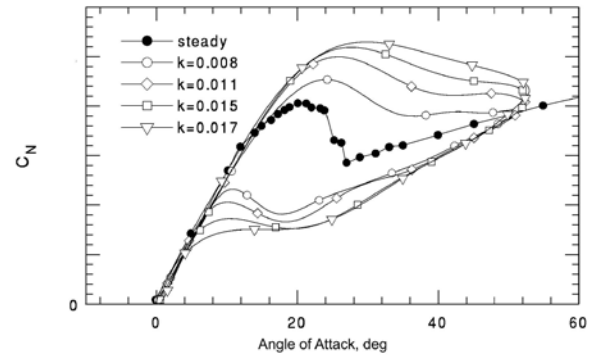


Figure 4. Normal force at stall conditions: static (filled circles) and dynamic dependencies (empty markers).

B. Analytic approximations

Multidimensional dependencies of aerodynamic coefficients obtained in rotary balance (RB) tests and represented in the form of look-up data tables are approximated by the polynomial expansion ($i = X, Y, Z, l, m, n$)

$$C_{iRB}(\alpha, \beta, \omega) = C_{i0}(\alpha) + C_{i\beta}(\alpha)\beta + C_{i\omega}(\alpha)\omega + C_{i\beta\omega}(\alpha)\beta\omega + C_{i\beta^2}(\alpha)\beta^2 + C_{i\omega^2}(\alpha)\omega^2 + C_{i\beta\omega}(\alpha)\beta\omega + C_{i\beta^3}(\alpha)\beta^3 + C_{i\beta^2\omega}(\alpha)\beta^2\omega + C_{i\beta\omega^2}(\alpha)\beta\omega^2 + C_{i\omega^3}(\alpha)\omega^3 \quad (1)$$

which helps to separate the aerodynamic asymmetry, linear aerodynamic autorotation and nonlinear terms. Accuracy of this approximation is shown in Fig. 5 (dashed lines - experimental data, solid lines - polynomial expansion). To accommodate the outlined aerodynamic effects in the aerodynamic model the wind axes projections of angular velocity p_a, q_a, r_a are used instead of body axes angular rates p, q, r (see Fig. 1). This allows direct use of aerodynamic dependencies obtained in the rotary balance tests (note that $p_a = \omega$):

$$\begin{aligned}
 p_a &= p \cos \alpha \cos \beta + r \sin \alpha \cos \beta + q \sin \beta \\
 r_a &= p \sin \alpha - r \cos \alpha \\
 q_a &= -p \cos \alpha \sin \beta - r \sin \alpha \sin \beta + q \cos \beta
 \end{aligned} \tag{2}$$

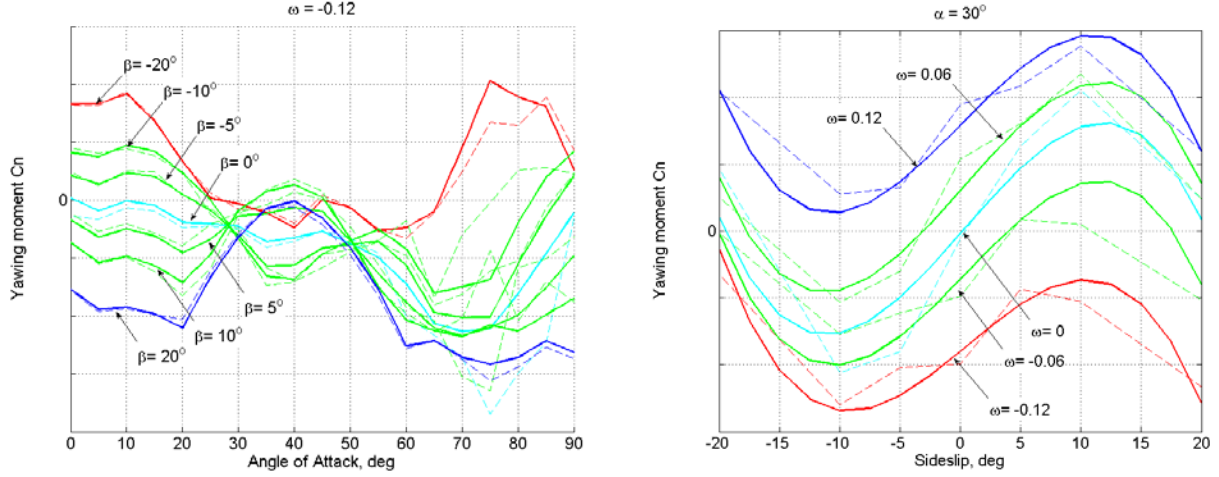


Figure 5. Yawing moment coefficient vs angle of attack α , sideslip β and nondimensional rate of rotation ω .

The following assembly of the aerodynamic model is applied using the aerodynamic data from static (ST), forced oscillation (FO) and rotary balance (RB) tests ($i = X, Y, Z, l, m, n$)

$$C_i = C_{iST}(\alpha, \beta) + \Delta C_{iRB}(\alpha, \beta, p_a) + \Delta C_{iST}(\alpha, \delta) + C_{i q_a FO}(\alpha) q_a + C_{i r_a FO}(\alpha) r_a \tag{3}$$

Aerodynamic derivatives in (3) with respect to q_a and r_a angular rates are calculated from the aerodynamic derivatives obtained in forced oscillation tests with respect to body axes angular rates p, q, r .

To extrapolate the aerodynamic dependencies on Mach number to higher angles of attack in a corner area of the available experimental data the following functional approximation is used (the lift coefficient is considered as an example):

$$C_L(\alpha, M) = C_{L0}(M) + k_1(M) \cdot C_{L(M=0.4)}(k_2(M) \cdot \alpha) \tag{4}$$

where $C_{L0}(M)$ is the dependence of the lift coefficient at zero incidence, $C_{L(M=0.4)}(\alpha)$ is the experimental dependence of the lift coefficient at $M = 0.4$, $k_1(M)$ and $k_2(M)$ are identified to approximate experimental dependencies at different Mach numbers. In fact, only coefficient $k_1(M)$ should be identified since $k_1(M)$ and $k_2(M)$ are not independent:

$$k_1(M) = \frac{C_{L\alpha}(M)}{C_{L\alpha}(M=0.4) \cdot k_2(M)} \tag{5}$$

The accuracy of approximation (5) is shown in Fig. 3. Decoupling functional approximation for Mach number and angle of attack dependencies similar to (4) and (5) are applied in the SUPRA extended aerodynamic model for all longitudinal and lateral/directional aerodynamic coefficients.

C. Unsteady aerodynamic model

Unsteady aerodynamic effects at stalled conditions require implementation of a special modeling approach³. The unsteady aerodynamic contribution may be represented as additional aerodynamic term in (3), for example, as follows

$$C = C(\alpha, \delta) + C_{dyn}(t) \tag{6}$$

where the time dependent component in (6) is described by the ordinary differential equation shown below as a washout filter

$$C_{dyn} = \frac{\tau s}{\tau s + 1} \Delta C(\alpha) \quad (7)$$

where τ is the characteristic time scale of separated flow development. Note that in static conditions term C_{dyn} gives zero contribution to the total aerodynamic load. The aerodynamic model incorporates unsteady nonlinear variations of type (7) in the lift and pitching moment coefficients.

D. Complementary use of CFD

The SUPRA aerodynamic model developed based on experimental wind tunnel data includes a number of reconfigurable parameters. They need to be tuned to produce a representative airplane behavior at stall and beyond stall conditions, which will be positively accepted by expert pilots. CFD capabilities available at NLR were used for evaluation of Reynolds number effects on dynamic stall, aerodynamic autorotation and onset of asymmetry. These results allowed to tune the SUPRA model reconfigurable parameters within justifiable physical limits.

CFD method: NLR's CFD solver ENSOLV is employed as the CFD method¹⁰. ENSOLV is based on a multi-block structured grid to give the solution of the Navier-Stokes equations. There are two modes involved in the present investigation, namely the Reynolds-Averaged Navier-Stokes (RANS) mode and the hybrid RANS/LES mode (Large Eddy Simulation). In the RANS mode, the Turbulence Numerics Team (TNT) formulation of the $k-\omega$ turbulence model is applied¹¹.

In the hybrid RANS/LES mode, the X-LES¹² formulation is applied. X-LES is a particular DES method¹³ that consists of a composition of a RANS $k-\omega$ turbulence model and a k -equation SGS model. Both the RANS $k-\omega$ model and the k -equation SGS model use the Boussinesq hypothesis to model the Reynolds or subgrid-scale stress tensor, which depends on the eddy-viscosity coefficient ν_t . Both models are based on the equation for the modeled turbulent kinetic energy k , which depends on its dissipation rate ε . Both the eddy viscosity and the dissipation rate are modeled using the turbulent kinetic energy as velocity scale together with a length scale l_t ,

$$\nu_t = l_t \sqrt{k} \quad \varepsilon = \beta_k \frac{k^{3/2}}{l_t}$$

where l_t is defined as a combination of the RANS length scale $l = \sqrt{k}/\omega$ and the SGS filter width Δ ,

$$l_t = \min\{l, C_1 \Delta\}$$

with $C_1 = 0.05$. The RANS $k-\omega$ model is completed by an equation for the specific dissipation rate ω and uses the TNT set of coefficients. The X-LES method will be in LES mode when the filter width (times C_1) is small compared to the RANS length scale. Note that in that case the SGS model is completely independent of ω .

Geometry and grid: The baseline T-tail configuration of the NACRE aircraft¹⁴ is used as a means to generate the high angles of attack flow phenomena. Fig. 7 gives an illustration of the aircraft geometry and implemented grid. A multi-block structured grid is generated around the complete aircraft configuration. For affordability, the so-called medium grid resolution consisting of about 4.2 million cells is used to generate the flow solutions. The grid is appropriately stretched

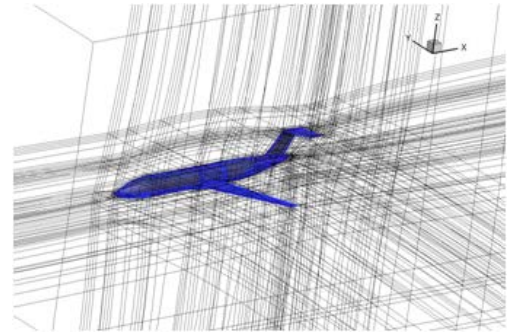


Figure 3. NACRE model geometry and grid

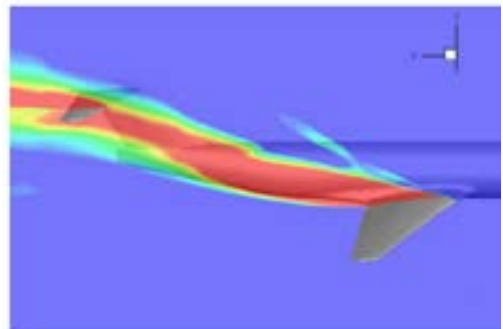
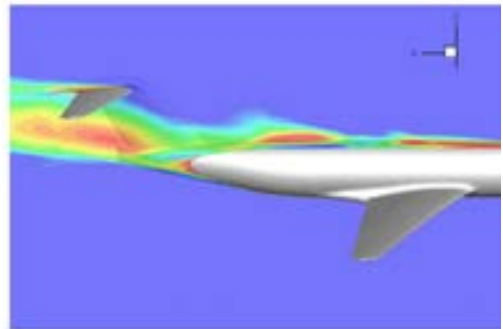


Figure 8. Wing-tail interaction for different angles of attack.

towards the solid wall to sufficiently resolve the boundary layer by the value of y^+ of around unity. Fig. 8 shows examples of flow visualization for separated from the wing wake interacting with T-tail for two different angles of attack.

Aerodynamic autorotation: The most significant issue in using wind tunnel aerodynamic data for simulation of airplane dynamics at stall conditions is the discrepancy of Reynolds number between the wind tunnel tests ($Re \approx 1.0 \cdot 10^6$) and full-scale airplane ($Re \approx 20 \cdot 10^6$). Separated flow from the wing is strongly affected by increase of Reynolds number leading to significant increase in the magnitude and angle of attack for the maximum lift. Normally with increase of angle of attack the variation of lift is negative immediately beyond maximum lift. In free flight the down-going wing will experience a loss of lift, further increasing the tendency for the wing to drop and resulting in a pro-spin propelling rolling moment known as wing autorotation. An intensity of aerodynamic autorotation and angle of attack range where it takes place similarly to the lift case should strongly depend on Reynolds number. As a result the prediction of airplane flight characteristics near and above stall will strongly depend on Reynolds number effect. One can expect that increase in Reynolds number at full-scale airplane will lead to more intensive post-stall departure, more dangerous spin at higher angles of attack and unsatisfactory spin recovery⁴.

To evaluate the fidelity of the wind tunnel data for autorotation a CFD assessment of the autorotation characteristics was conducted through computation of aerodynamic loads at coning motion with different roll-rates.

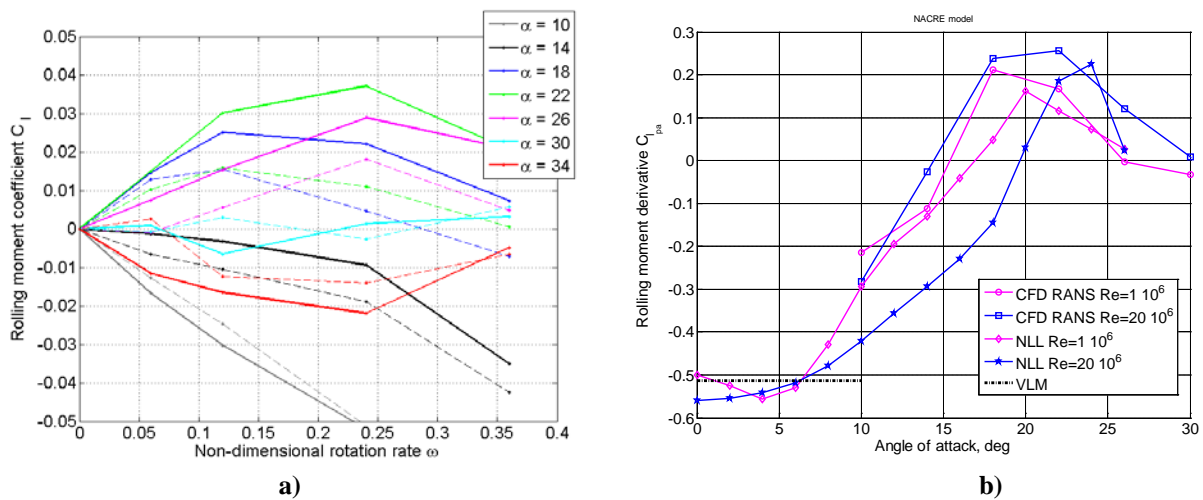


Figure 8. a) CFD computation of the rolling moment $C_l(\alpha, \omega)$ (solid lines $Re=20 \cdot 10^6$, dashed lines $Re=1 \cdot 10^6$). b) Derivative $C_{l\omega}(\alpha, \omega = 0)$ - CFD vs low order methods (Prandtl's Nonlinear Lifting Line, NLL, and Vortex lattice Method, VLM). NACRE model.

Two approaches have been used. The first approach employs a time-accurate simulation, where a time-averaged force and moment coefficients are obtained by averaging the time-accurate data. The second approach is an approximate one, using a steady-state simulation. In the latter case, the force and moment coefficients are obtained by averaging the alternating values of the force and moment coefficients from a non-converged steady-state solution. Both approaches use the RANS modeling. Apparently, the second approach is more economical in terms of computational resource. It requires a fraction of CPU time. Although it gives only approximative results, in some cases it can produce the phenomenological trends in a level of approximation that is sufficient for the purpose of aerodynamic modeling.

Aerodynamic autorotation for NACRE model was evaluated at two Reynolds numbers corresponding to wind tunnel and full-scale airplane conditions, $Re = 1 \cdot 10^6$ and $Re = 20 \cdot 10^6$, respectively (see Fig. 8a,b).

Increase of Reynolds number from wind tunnel to full-scale flight conditions significantly increases the pro-spin autorotation rolling moment C_l . For example, at $\alpha = 22^\circ$ the maximum magnitude of the pro-spin rolling moment coefficient at $Re = 20 \cdot 10^6$ is approximately two times bigger than at $Re = 1 \cdot 10^6$ (Fig. 8a). This difference may be attributed to the possibility that in real flight the level of aerodynamic asymmetry in roll may be more than two times higher. Aerodynamic derivative $C_{l\omega}(\alpha, \omega = 0)$ is responsible for the lateral/directional instability, which leads to post-stall departure. In Fig. 8b this derivative is presented in comparison between CFD prediction and predictions

made using simple low order aerodynamic models, the Prandtl Nonlinear Lifting Line (NLL) theory and Vortex Lattice Method (VLM)¹⁵. At low Reynolds number CFD and NLL predictions are reasonably close, at high Reynolds number NLL gives delay in onset of autorotation in angle of attack on about five degrees.

Evaluation of dynamic hysteresis: CFD modeling results for the normal force in static conditions (black solid line) and at periodical variation of angle of attack $\alpha = 16^\circ + 10^\circ \sin 2\pi ft$ (blue solid line) with frequency $f = 0.35Hz$ are presented in Fig. 9. These results reveal a significant hysteresis loop in variation of the force coefficient. Similar result can be modeled using a phenomenological model of type (6), (7). After identification of the phenomenological model parameters, i.e. the characteristic time constant ($\tau = 0.1sec$) and nonlinear function $\Delta C(\alpha)$, the predicted variation of the normal force coefficient (red dashed line in Fig. 9) is quite close to the CFD hysteresis loop.

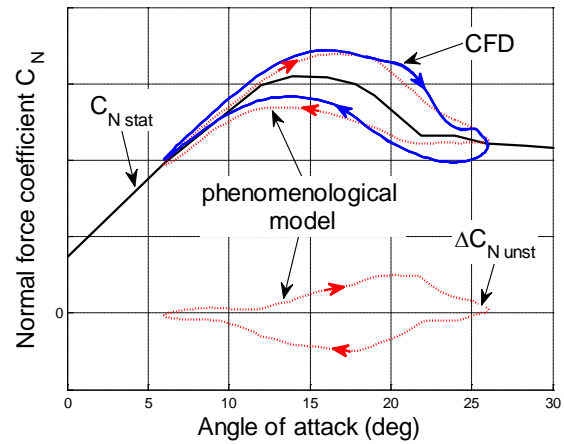


Figure 9. Phenomenological unsteady aerodynamic model (6), (7) vs CFD simulation.

E. Command stability augmentation system

The SUPRA simulation model in block-diagram in Fig. 1 includes a basic command and stability augmentation system (CSAS) for providing airplane required controllability and stability characteristics for normal flight regimes. In the longitudinal channel the aircraft is controlled by means of elevator and stabilizer. The stabilizer is used only for trimming purposes and is deflected slowly. The required elevator deflection is defined by pilot longitudinal control input X_{lon} and feedback signals including terms proportional to the pitch rate and the normal load factor n_z . A nonlinear correction is used to compensate nonlinearity in the pitching aerodynamic moment in the pre-stall region of angles of attack. Euler’s angles are used for compensation of gravity terms.

The lateral/directional channels are controlled by means of rudder, ailerons and interceptors. Rudder is deflected proportionally with pedals X_{ped} and yaw rate signal sent through a washout filter. There is also an interconnect with lateral control input X_{lat} . Aileron deflection is proportional to the lateral control input X_{lat} . Interceptors are helping ailerons to improve controllability in roll, they are deflected when lateral control input exceeds some amplitude $|X_{lat}| > X_{lat*}$

F. Propulsion model

The aircraft has two turbofan engines with thrust characteristics described by the look-up data tables depending on altitude, Mach number and throttle position. Dynamic characteristics of engines such as delay in response to throttle input and thrust increase/decrease rate limit are simulated by the second order dynamical system with saturation nonlinearities.

G. Buffeting model

Aerodynamic buffeting of the airframe at high angles of attack was simulated by shaking the cockpit with a simulator driving mechanism (Fig. 1). The buffet intensity and frequency content were controlled by the computer, with the buffet amplitude gradually increasing with angle of attack. Buffet onset occurs after exceeding some critical angle of attack which varies with Mach number (green line in Fig. 10 top). The intensity of buffet is increasing fairly linearly thereafter with increasing angle of attack. The frequency content of the three

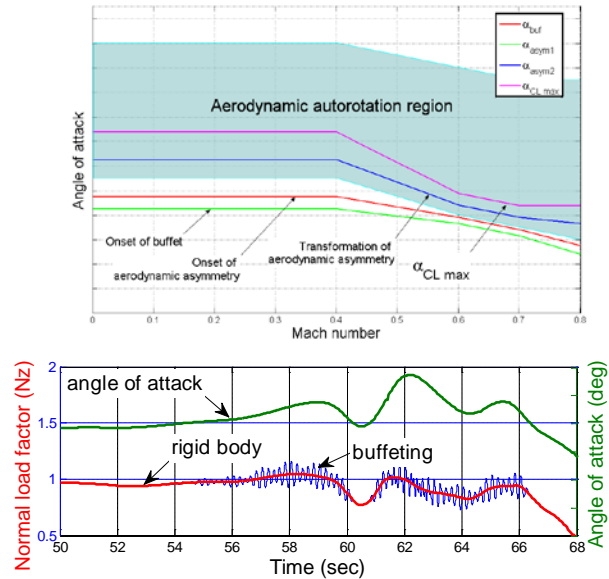


Figure 10. Onset boundaries for buffeting, aerodynamic asymmetry and autorotation in roll.

structural modes was selected to represent buffet observed in flight tests and taking into account driving system capability. Fig. 10 top shows also boundaries for onset and transformation of the rolling moment asymmetry and the region of aerodynamic autorotation. Example of buffeting (blue line) as an increment to the rigid body normal load factor (red line) is shown in Fig. 10 along with variation of angle of attack.

III. Nonlinear Dynamics Analysis

A. Departure Criteria

A systematic analysis of the SUPRA model nonlinear flight dynamics has been conducted to investigate a variety of airplane critical flight regimes^{16,17,18}. This is considered as an important part of the validation process and also as a platform for planning piloted simulation scenarios for upset recovery training. This study highlighted potential dangers of airplane departure, the character of post-stall gyration, incipient/developed spin modes and high speed steep spiral dive. A special study was made to investigate effect of free parameters introduced in the aerodynamic model on airplane nonlinear dynamics, namely the post-stall lateral/directional departure and longitudinal deep-stall regimes.

The intensity of aerodynamic autorotation in the SUPRA aerodynamic model, namely derivative $C_{l\omega}(\alpha)$ obtained in wind tunnel rotary balance tests, due to uncertainty of Reynolds number effect was parameterized. The transformation of the rotary derivative $C_{l\omega}(\alpha)$ was made using a spline function defined in angle of attack range specific for onset of aerodynamic autorotation and scaled by a number of parameter. These parameters allow one to shape the autorotation effect to meet desired lateral/directional departure behavior. An approximate departure criterion for lateral/directional departure

$$C_{n\beta_{dyn}}(\alpha) = C_{n\beta}(\alpha)\cos\alpha - \frac{l_z}{l_x}C_{l\beta}(\alpha)\sin\alpha < 0 \quad (8)$$

was very successful in departure prediction for combat aircraft with small aspect ratio wing¹⁵. Combat aircraft departure is provoked by intense vortices and their asymmetrical breakdown over the wings at high angles of attack. Lateral/directional departure of a generic transport airplane is provoked by asymmetrical flow separation over the wings and in this case the criterion (8) does not work in stall region. Another criterion for prediction of post-stall departure is required¹⁶:

$$\sigma_\omega(\alpha) = C_{n\beta}(\alpha)C_{l\omega}(\alpha) - C_{l\beta}(\alpha)C_{n\omega}(\alpha) > 0 \quad (9)$$

where $C_{l\beta}(\alpha)$, $C_{n\beta}(\alpha)$ – the aerodynamic derivatives obtained in static tests, and $C_{l\omega}(\alpha)$, $C_{n\omega}(\alpha)$ – the aerodynamic

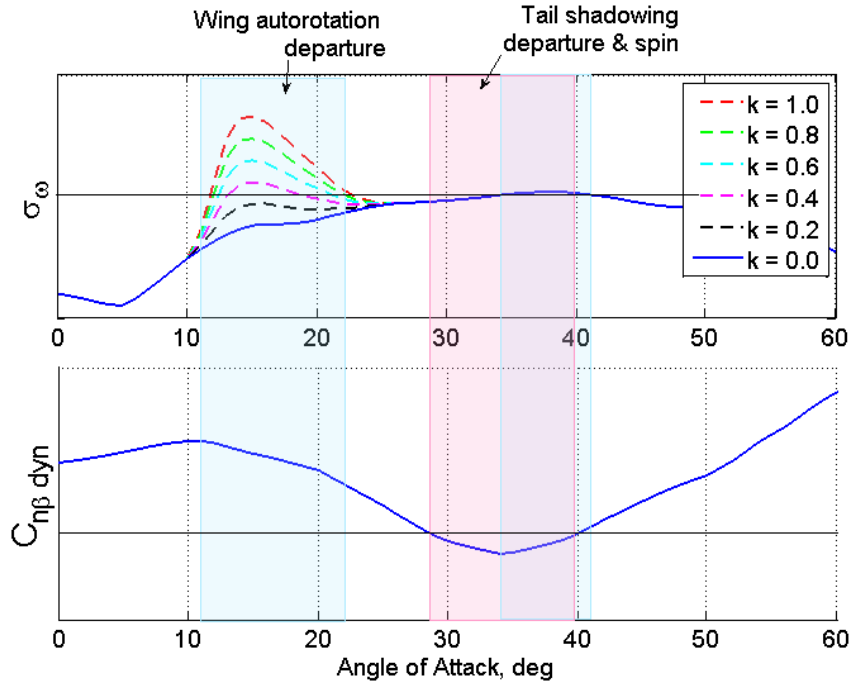


Figure 11. Lateral/directional departure criteria.

rotary derivatives obtained in rotary balance tests.

Fig. 11 shows departure criteria (8) and (9) for the SUPRA aerodynamic model. Criterion (8) indicates instability in lateral/directional motion at angles of attack $\alpha \cong (28^0, 40^0)$ well above the stall region. This instability can be attributed to the vertical tail shadowing by wings and fuselage. Nonlinear dynamics analysis presented in the next section shows that this instability leads to developed spin modes at $\alpha \approx 40^0$, which are supported by nonlinear dependencies similar to ones shown in Fig. 5. Criterion (9) was parameterized by coefficient $k \in (0,1)$. The case $k = 0$ corresponds to the wind tunnel data, when derivative $C_{l\omega}(\alpha) > 0$ is not sufficient for onset of lateral/directional departure. The case $k = 1$ corresponds to the maximum justifiable level of aerodynamic autorotation evaluated in CFD investigation for real flight Reynolds numbers. Fig. 11 shows how the intensity and angle of attack range for departure parameter σ_ω (9) can be transformed by parameter k .

B. Nonlinear bifurcation analysis

Approximate linear criteria (8) and (9) indicate onset of local instability in the lateral/direction motion. Nonlinear analysis is required to highlight how this instability will progress and what is a new attractor in nonlinear aircraft dynamics. On a short time interval this analysis can be performed considering simplified equations of motion when

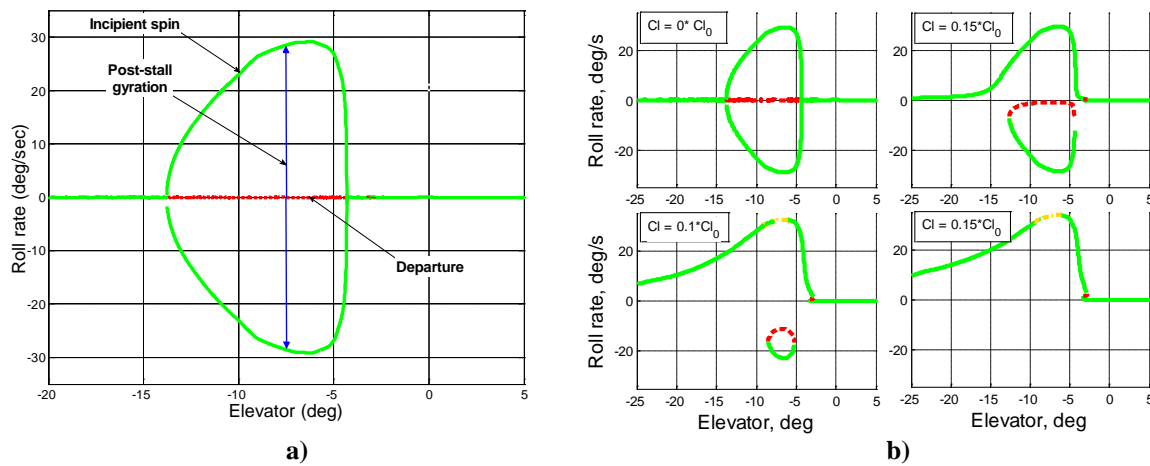


Figure 12. a) Autorotation bifurcation; b) Structural instability of autorotation bifurcation ($k = 0.4$).

speed is constant, $V = const$, and effect of gravity is neglected, i.e. $g = 0$. The results of bifurcational analysis of the SUPRA open airframe at $k = 0.4$ are shown in Figs. 12a and 12b. The structure of autorotation bifurcation includes two pitch-fork bifurcation points at $\delta_e = -4^0$ and $\delta_e = -13.5^0$ bounding the segment of unstable equilibria at zero rotation (dashed red line on Fig. 12a). Two-sided stable equilibrium branches with non-zero rotation are connecting the pitch-fork bifurcation points. There is a clear physical interpretation of this bifurcation diagram in terms of flight dynamics phenomena. The aperiodically unstable branch (dashed red segment) signifies lateral/directional departure predicted by approximate criterion (9). Post-stall gyration is equally possible to positive or negative direction and it is described by transitional motion from unstable symmetrical flight to autorotation stable regime (green curved lines). Post-stall gyration following departure event is approaching incipient spin modes described by the two stable autorotation branches (two green curved lines connecting bifurcation points).

The bifurcation diagram in Fig. 12a corresponds to symmetrical case when the rolling moment at zero rotation and sideslip equals to zero. Onset of aerodynamic asymmetry in addition to aerodynamic autorotation transforms the bifurcation diagram as shown in Fig. 12b. The pitch-fork bifurcation point is structurally unstable under small perturbations of the system. Even micro asymmetry transforms symmetrical diagram into two disconnected branches. One branch includes all stable equilibrium states and the second one is the closed-loop disconnected branch which includes stable and unstable parts. Further increase of aerodynamic asymmetry totally eliminates the closed-loop branch and all equilibrium states are stable and one-sided. The magnitude of roll asymmetry when the closed-loop equilibrium branch disappears is relatively small with respect to selected in SUPRA model level of asymmetry. The analysis presented above helps to understand the topology of equilibrium solutions in nonlinear aircraft dynamics and useful for shaping the required post-stall behaviors.

Figs. 15 and 16 show results of continuation and bifurcation analysis of all possible equilibrium states in the full set of aircraft nonlinear equations for open airframe and for SUPRA model with CSAS, respectively. Six motion parameters $\alpha, \beta, p, V, \theta, \phi$ in equilibrium flight, which is a helical trajectory with vertical axis, are shown as function of elevator deflection δ_e in Fig. 15 and as function of longitudinal stick deflection X_{lon} in Fig. 16. Different parts of equilibrium branches are marked by different colors to indicate local stability characteristics: green color marks stable equilibrium points, red color marks aperiodically unstable equilibrium states with one positive real eigenvalue, yellow color marks oscillatory unstable equilibrium states with one unstable complex-conjugate pair of eigenvalues. Other colors signify equilibrium states with instability of higher order.

All continuation and bifurcation diagrams for motion parameters in Figs. 15 and 16 are supplied with specifications of the equilibrium branches, arrows show equilibrium states which are approached after post-stall gyration. The green lines show a stable branch with normal flight regimes. The pitch-up deflection of elevator leads to onset of lateral directional departure (red dashed lines) and post-stall gyration to a steep spiral dive or to a helical trajectory. Steep spiral dive is very dangerous as speed increases to $V = 250 \text{ m/s}$ and normal load factor $n_z \approx 4.5$. Transition to a spiral trajectory at $\delta_e < -10^\circ$ is less dangerous. There is also a developed spin mode possible at all elevator deflection with parameters $\alpha \approx 40^\circ, \beta \approx 9^\circ, p \approx 40 \text{ deg/s}, V \approx 135 \text{ m/s}$, etc. The steep spiral dive modes in the case of SUPRA model with CSAS (see Fig. 16) are eliminated and the remaining helical trajectories are slightly transformed having a larger radius and slower rotation rate.

The presented in Figs. 15 and 16 continuation and bifurcation diagrams correspond to maximum level of aerodynamic autorotation at $k = 1$, which was selected by experienced test pilot during SUPRA model validation and parameters tuning. A brief outline of the piloted validation process is given in the next section.

IV. Aerodynamic model validation and parameters tuning

The piloted evaluation had two primary goals: a) establish that the behavior of the generic, class-specific aircraft model developed by SUPRA is representative of the aircraft class inside and outside the normal flight envelope; b) demonstrate that improvements to motion cueing are feasible on conventional, hexapod-type devices as well as to show that advanced, centrifuge-based platforms provide an improvement over conventional devices. The following discussion of the piloted evaluation trials will focus on the efforts in support of goal a).

A. Methods

Even though the simulation model developed by SUPRA is generic, i.e. no real aircraft exists that the simulation behavior could be matched to, it has to comply with general handling requirements for this class of airplane and should meet test pilot expectations for the flying qualities of an airplane of the class: operating weight approx 94t, max. thrust about 2x33k lbf, stall speed (1g, clean): 175 kts, V_{mo}/M_{mo} : 330kts/.82, column/wheel manipulator, conventional flight controls. The "Qualification" of the SUPRA model for the remainder of the evaluation program was based on this assumption. Consequently only test pilots with experience in certification programs as well as flight of commercial airplanes outside the normal envelope could be used for this part of the trials. After fine tuning of the simulation model on all three simulator facilities, NLR's Grace, TNO's Desdemona and TsAGI's PSPK-102, which was largely performed with the help of Distinguished Test Pilot Vladimir Biryukov, the qualification of the model started with European, Russian and U.S. pilots. 10 Pilots were available at the DESDEMONA facility, 9 at the Grace simulator, and 2 at TsAGI.

Evaluation of the model behavior was performed inside as well as outside the normal envelope. Both evaluations comprised a guided free flight phase and a scenario phase. During the guided free flight phase a set of maneuvers was carried out at different altitudes and airspeeds to evaluate aircraft response as acceptable or non-acceptable. The following characteristics were rated for behavior inside the normal envelope (2 altitudes: FL130 and FL350, and 3 airspeeds: 1.2 Vs, 270kts, V_{mo}/M_{mo}):

- Airplane trim from Vls up to V_{mo}/M_{mo}
- Pitching moment due to thrust
- Phugoid stability
- Dutch roll (magnitude and phase)
- Pitch response
- Roll response
- Yaw response
- Steady side slip/roll angle
- Acceleration and deceleration
- Flight with asymmetric thrust
- Control force, roll
- Column force per g / force gradient

For non-normal maneuvers the following characteristics were rated by the pilots (Approach to Stall and Stall at 10k ft and 30k ft):

- Loss of roll controllability with increasing AoA
- CS25 Stall: Lateral instabilities approaching stall
- Accelerated stall: lateral instabilities approaching stall
- Accelerated stall: Buffet – onset

- CS25 Stall: Buffet – onset
- CS25 Stall: Buffet – Magnitude and frequency
- CS25 Stall: Stick shaker onset
- CS25 Stall: Stall – roll-off: onset AoA
- Accelerated stall: Buffet – Magnitude and frequency
- Accelerated stall: Stick shaker onset
- Accelerated stall: Stall – roll-off: onset AoA
- Accelerated stall: Stall – roll-off: roll rate

The scenario-based evaluation consisted of 3 unusual attitudes, nose high/wings level, nose high/high bank and nose low/high bank, which could be recovered remaining inside the normal aerodynamic envelope and a set of 18 approach-to-stall and stall scenarios at various levels of asymmetry, in straight and turning flight. Fig. 13 provides a more detailed break-down.

By performing the “build-up” described, i.e. going from single maneuvers to more dynamic and complex scenarios, the pilots were able to get a comprehensive picture of the model behavior. After finishing the maneuver-based and the scenario-based evaluation the pilots were asked to provide a general acceptability rating on a scale from 1 through 4; ratings 1 and 2 meaning acceptable behavior, a rating of 1 meaning fully representative of the airplane class. The rating scale is shown in Table 1 from¹. The acceptability ratings were provided for normal maneuvering and approach-to-stall/stall separately.

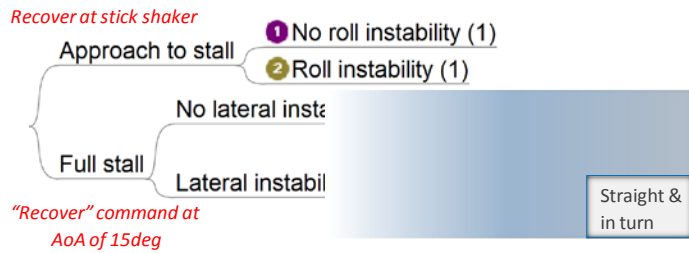


Figure 13. Scenarios for evaluation of stall behavior.

As the evaluation of the SUPRA motion cueing concepts was to follow the qualification of the simulation model it was decided to minimize the influence of motion on the handling evaluation. Hence, normal maneuvering trials were carried out without motion cueing and stall maneuvers were flown with onset cueing to provide stall buffet and a minimum of motion cues during stall departure.

B. Results

The vast majority of the ratings received from all pilots in the maneuver-based evaluation was *acceptable*, for both normal and stall maneuvering. Some of the consistent comments that were given by the pilots are presented below.

Normal maneuvers:

- Sensitive in roll
- Little phugoid/speed stability observable

Approach-to-stall/stall maneuvers:

- Very realistic buffet
- Nose-down/inherent unloading tendency is weak
- Lateral-directional instability excellent, not part of current simulation models

Fig. 14 depicts median and spread of the acceptability ratings received for the model on the centrifuge-based DESDEMONA simulator and the two hexapod platforms. As can be seen the ratings are in the *acceptable* region, with only few exceptions for the stall behavior on hexapod platforms. Median ratings on hexapod platforms are “1”, i.e. fully representative, with a slightly larger spread for stall regimes. On the DESDEMONA platform the median rating for normal maneuvers is largely representative (7 pilots gave a rating of “2”, 3 a rating of “1”), for stall maneuvers fully representative (3 pilots gave a rating of “2”, 7 pilots a rating of “1”).

Fig. 17 shows the example of piloted simulation results presented as classical time histories and also in the form of their phase portraits.

V. Conclusions

The SUPRA aerodynamic model for a generic large category transport aircraft allows simulation of multiple phenomena representative for stall/post-stall flight conditions. A combination of wind tunnel and CFD data allow reconfiguration of the SUPRA aerodynamic model parameters within justifiable physical limits. Validation and tuning of the SUPRA aerodynamic model included systematic computational investigation of nonlinear dynamics in extended flight envelope and piloted simulation. The piloted evaluation trials provided proof that the SUPRA model behavior is representative of a jet transport of conventional configuration and an operating weight of approx. 100 tons, inside and outside the normal flight envelope. Important arguments have been gathered in support of the usability of the phenomenological modeling approach for similar efforts. SUPRA provided evidence that the

method, which had previously been used successfully for the prediction of stall and spin behavior of advanced fighter jet configurations, is usable to produce an all-envelope class-representative model. The model's re-configurability allows for customization to reproduce certain more type-specific characteristics.

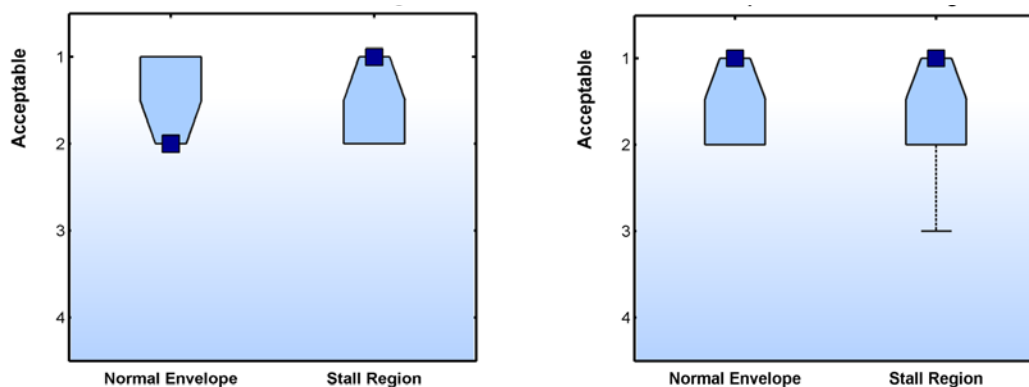


Figure 14. Box plots for received model ratings on DESDEMONA (left) and hexapod simulators (right).

Acknowledgments

The authors thank all pilots for their valuable contribution in the evaluation of the SUPRA simulation and the members of the SUPRA expert group for their useful guidance throughout the project. The project was funded by EC contract 233543.

References

- ¹Groen, E., Ledegang, W., Fucke, L., Nooij, S., Goman, M., Mayrhofer, M., Zaichik, L., Grigoryev, M., Biryukov, V. "SUPRA- Enhanced Upset Recovery Simulation", *AIAA Modeling, Simulation Technologies Conference*, Minneapolis, Minnesota, August 2012 (submitted for publication).
- ²Abramov, N.B., Goman, M.G., Khrabrov, A.N. and Soemarwoto, B. "Aerodynamic Model Development for Simulation of Upset Recovery of Transport Airplane", *RAeS Aerodynamic Conference – Applied Aerodynamics: Capabilities and Future Requirements*, London, 27-28 July 2010.
- ³Khrabrov, A., Sidoryuk, M., Goman, M., "Aerodynamic Model Development and Simulation of Airliner Spin for Upset Recovery", *4th European Conference for Aerospace Sciences EUCASS*, St Petersburg, July 4-8, 2011.
- ⁴Chambers, J.R. Modeling Flight: The Role of Dynamically Scaled Free-Flight Models in Support of NASA's Aerospace Programs. NASA SP 2009-575.
- ⁵Biryukov V., Fucke L., Grigoriev M., Groen E., et al. Developing Scenarios for Research into Upset Recovery Simulation AIAA-2010-7794, *AIAA Modeling and Simulation Technologies Conference*, Toronto, ON, 2-5 August 2010.
- ⁶Foster, J.V., Cunningham, K., Fremaux, Ch.M., Shah, G.H., Stewart, E.C., Rivers, R.A., Wilborn, J.E., Gato, W. Dynamics Modeling and Simulation of Large Transport Airplanes in Upset Conditions. AIAA-2005-5933, *AIAA Atmospheric Flight Mechanics Conference and Exhibit*, 15-18 August 2005, San Francisco, California.
- ⁷Cunningham, K., Foster, J.V., Shah, G.H., Stewart, E.C., Ventura, R.N., Rivers, R.A., Wilborn, J.E., Gato, W. Simulation Study of Flap Effects on a Commercial Transport Airplane in Upset Conditions. AIAA-2005-5908, *AIAA Atmospheric Flight Mechanics Conference and Exhibit*, 15-18 August 2005, San Francisco, California.
- ⁸Gingras, D.R. and Ralston, J.N. Improvement of Stall-Regime Aerodynamics Modeling for Aircraft Training Simulations. AIAA-2010-7793, *AIAA Modeling and Simulation Technologies Conference*, Toronto, ON, 2-5 August 2010.
- ⁹Khrabrov, A.N., Vinogradov, Yu.N. and Abramov, N.B. "Mathematical Modelling of Aircraft Unsteady Aerodynamics at High Incidence with Account of Wing-Tail Interaction", AIAA-2004-5278, *AIAA Atmospheric Flight Mechanics Conference and Exhibit*, Providence, Rhode Island, August 2004.
- ¹⁰Kok, J.C., Boerstol, J.W., Kassies, A. and Spekrijse, S.P. A Robust Multi-Block Navier-Stokes Flow Solver for Industrial Applications. *Proceedings of ECCOMAS Conference*, Paris, 1996 (also NLR-TP-96323, 1996).
- ¹¹Kok, J.C. Resolving the dependence on free stream values for the $k-\omega$ turbulence model. *AIAA Journal*, 38(7), pp. 1292-1294, 2000.
- ¹²Kok, J.C., Dol, H.S., Oskam, B. and van der Ven. Extra-large eddy simulation of massively separated flows. AIAA-2004-264, *42nd AIAA Aerospace Sciences Meeting*, Reno, NV, 5-8 January 2004

¹³Spalart, P.R., Jou, W.-H., Strelets, M. and Allmaras, S.R. (1997) Comments on the feasibility of LES for wings, and on a hybrid RANS/LES approach. In C.Liu and Z.Liu, Editors, *Advances in DNS/LES*. Greyden Press. Proc. 1st AFOSR Int. Conf. on DNS/LES, Ruston (LA), 1997.

¹⁴Schmollgruber, P. and Jentink, H. A multidisciplinary flying testbed for new aircraft concepts. Proceedings of 27th ICAS Congress, Nice, Sept. 2010, p.6.9.2.

¹⁵Khrabrov, A., "Computation of Aerodynamic Autorotation regions for High Aspect Ratio Wing", 6th *International Conference on Mathematical Problems in Engineering and Aerospace Sciences*, Edited by Seenith Sivasundaram, 2007 Cambridge Scientific Publishes.

¹⁵Maneuvre Limitations of Combat Aircraft. *AGARD Advisory Report No. 155A*, AGARD 1979.

¹⁶Goman, M.G., Zagainov, G.I., and Khrantsovsky, A.V. "Application of Bifurcation Methods to Nonlinear Flight Dynamics Problems". *Progress in Aerospace Sciences* 33, pp. 539-586, 1997, Elsevier Sciences, Ltd.

¹⁷Goman, M.G., and Khrantsovsky, A.V., "Computational Framework for Investigation of Aircraft Nonlinear Dynamics", *Journal Advances in Engineering Software*, Vol. 39, Issue 3, March 2008, pp. 167-177.

¹⁸Kolesnikov, E., Goman, M., "Analysis of Aircraft Nonlinear Dynamics Using Non-Gradient Based Numerical Methods and Attainable Equilibrium Sets", *AIAA Atmospheric Flight Mechanics Conference*, Minneapolis, Minnesota, August 2012 (submitted for publication).

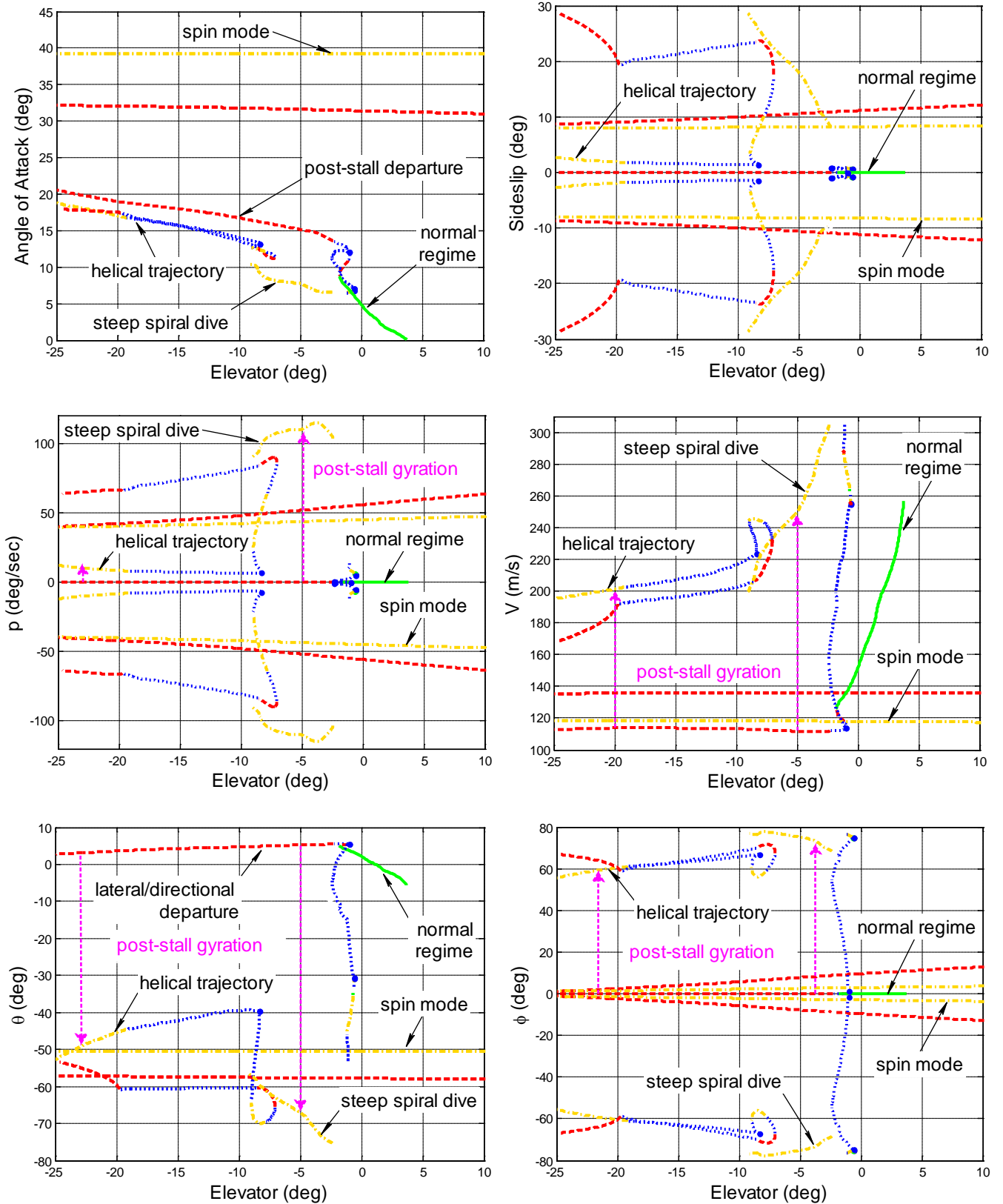


Figure 15. Continuation and bifurcation diagrams for the SUPRA open airframe.

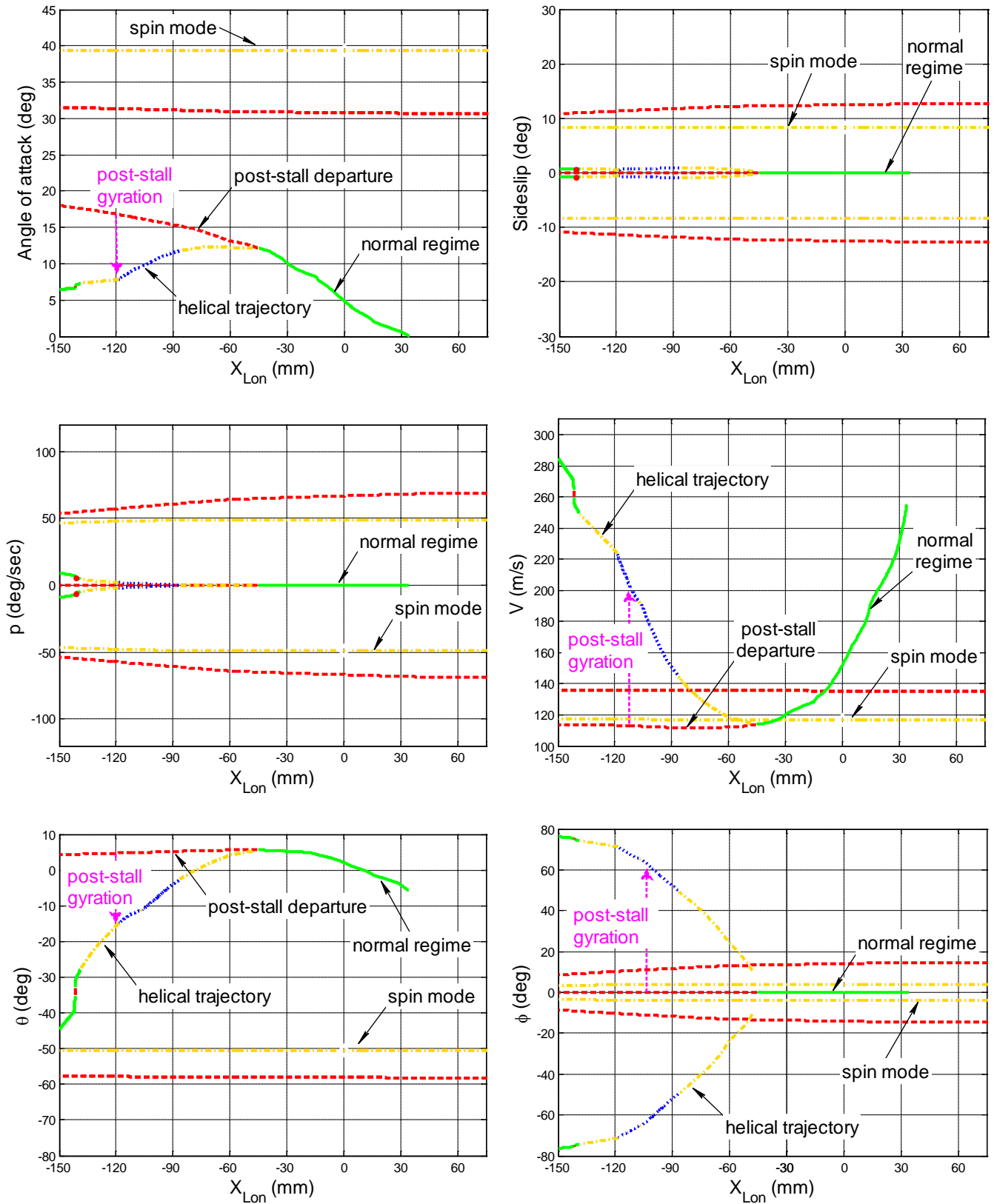


Figure 16. Continuation and bifurcation diagrams for the SUPRA closed-loop system.

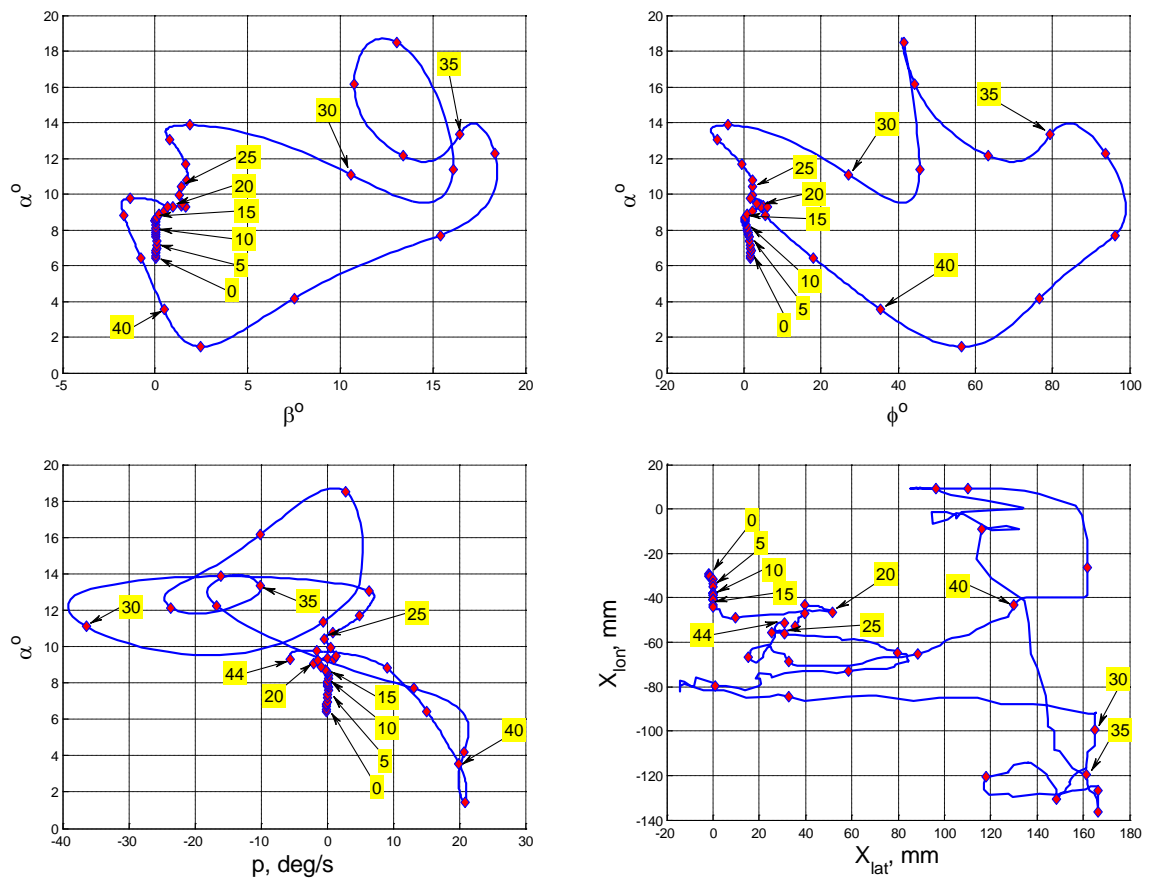
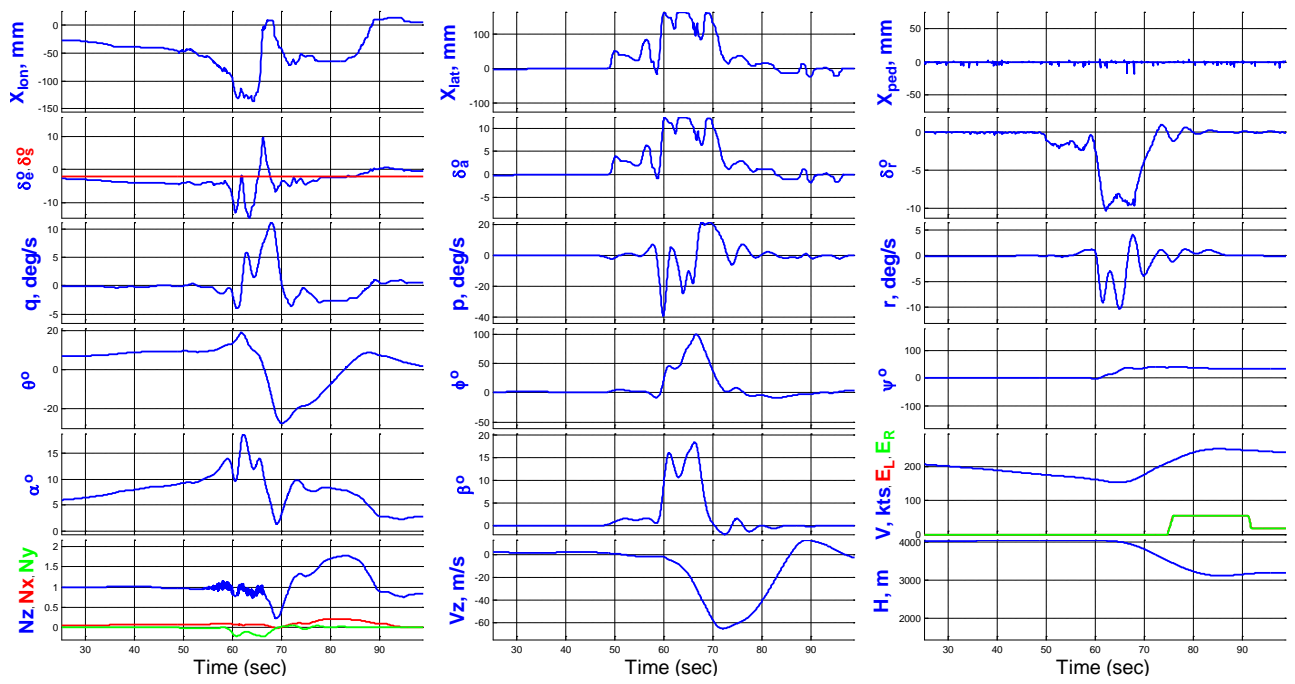


Figure 17. Piloted simulation time histories and their phase portraits.

This page is intentionally left blank.

NLR

Anthony Fokkerweg 2

1059 CM Amsterdam, The Netherlands

p) +31 88 511 3113 f) +31 88 511 3210

e) info@nlr.nl i) www.nlr.nl